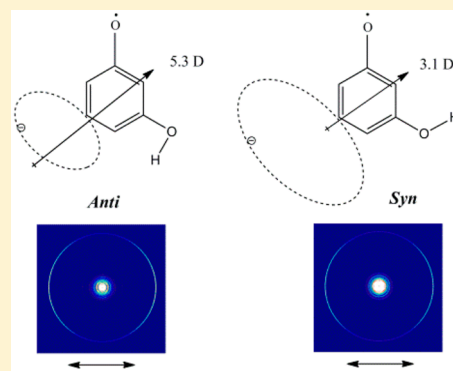


## Conformation-Selective Resonant Photoelectron Spectroscopy via Dipole-Bound States of Cold Anions

Dao-Ling Huang,<sup>†</sup> Hong-Tao Liu,<sup>‡</sup> Chuan-Gang Ning,<sup>§</sup> and Lai-Sheng Wang<sup>\*,†</sup><sup>†</sup>Department of Chemistry, Brown University, Providence, Rhode Island 02912, United States<sup>‡</sup>Shanghai Institute of Applied Physics, Chinese Academy of Sciences, Shanghai 201800, China<sup>§</sup>Department of Physics, State Key Laboratory of Low-Dimensional Quantum Physics, Tsinghua University, Beijing 100084, China

## Supporting Information

**ABSTRACT:** Molecular conformation is important in chemistry and biochemistry. Conformers connected by low energy barriers can only be observed at low temperatures and are difficult to be separated. Here we report a new method to obtain conformation-selective spectroscopic information about dipolar molecular radicals via dipole-bound excited states of the corresponding anions cooled in a cryogenic ion trap. We observed two conformers of cold 3-hydroxyphenoxide anions [*m*-HO(C<sub>6</sub>H<sub>4</sub>)O<sup>-</sup>] in high-resolution photoelectron spectroscopy and measured different electron affinities, 18 850(8) and 18 917(5) cm<sup>-1</sup>, for the *syn* and *anti* 3-hydroxyphenoxy radicals, respectively. We also observed dipole-bound excited states for *m*-HO(C<sub>6</sub>H<sub>4</sub>)O<sup>-</sup> with different binding energies for the two conformers due to the different dipole moments of the corresponding 3-hydroxyphenoxy radicals. Excitations to selected vibrational levels of the dipole-bound states result in conformation-selective photoelectron spectra. This method should be applicable to conformation-selective spectroscopic studies of any anions with dipolar neutral cores.



Molecular conformations play critical roles in chemistry and biochemistry. Many molecular conformers involve rotations of a functional group around a single covalent bond with low energy barriers. At room temperature, hindered rotations can occur, making it extremely difficult to separate molecular conformers. The cold environment in a supersonic molecular beam can cool molecules below the conformation barrier and has been used extensively for spectroscopic characterization of specific molecular conformers,<sup>1,2</sup> as well as investigations of conformer-specific photodissociation<sup>3,4</sup> and isomerization dynamics.<sup>5,6</sup> Additionally, cryogenic cooling in ion traps over the past decades<sup>7</sup> has allowed conformation-specific spectroscopy of molecular ions from electrospray ionization (ESI) sources.<sup>8</sup> Beyond spectroscopic and structural characterization, spatially separated conformers using inhomogeneous electric fields have been achieved for dipolar molecules,<sup>9</sup> enabling conformer-specific chemical reactions to be conducted.<sup>10</sup>

Molecules with sufficiently large dipole moments can form dipole-bound anions.<sup>11,12</sup> Stable anions can have dipole-bound excited states, if the corresponding neutral cores have large dipole moments.<sup>13</sup> The electron in the dipole-bound states (DBSs) is highly diffused with weak interactions with the neutral cores, analogous to Rydberg states of neutral molecules. Ro-vibrational excitations in the DBSs are sufficient to overcome the weak electron binding energies to induce autodetachment, which is evidenced as resonances in electron detachment cross sections<sup>13</sup> and has allowed high-resolution

detachment spectroscopy.<sup>14</sup> Recently, we have observed resonantly enhanced photoelectron spectroscopy (PES) due to mode- and state-selective autodetachment via vibrational levels of DBSs of several anions cooled in a cryogenic ion trap.<sup>15–19</sup> Significantly richer spectroscopic information about the underlying neutral radicals has been obtained from the resonantly enhanced PES than traditional PES. In particular, low frequency and Franck–Condon inactive vibrational modes have been observed.

Here we report a new method to obtain conformation-specific spectroscopic information on dipolar molecular radicals using resonant-enhanced high-resolution photoelectron (PE) imaging via DBSs of anions cooled in a temperature-controlled ion trap. The focus of the current work is the 3-hydroxyphenoxide anion [*m*-HO(C<sub>6</sub>H<sub>4</sub>)O<sup>-</sup>], which can have two stable conformers as shown in Figure 1. We have recently observed a DBS in the *o*-HO(C<sub>6</sub>H<sub>4</sub>)O<sup>-</sup> anion,<sup>18</sup> which is similar to *m*-HO(C<sub>6</sub>H<sub>4</sub>)O<sup>-</sup>, except that it has only one stable conformer. Our density functional theory (DFT) calculation at the B3LYP/6-311++G(d,p) level shows that the dipole moments of the *syn* and *anti* *m*-HO(C<sub>6</sub>H<sub>4</sub>)O• radical conformers are 3.1 and 5.3 D, respectively; both are large enough to support a DBS. As a matter of fact, the *syn* and *anti* conformers of a series of similar *meta*-substituted phenols (e.g.,

Received: May 9, 2015

Accepted: May 26, 2015

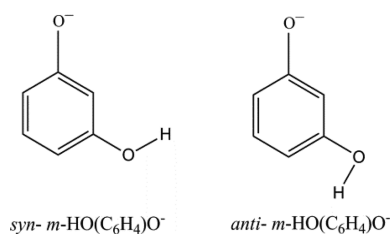


**Figure 1.** Schematic structures of the two conformers of  $m\text{-HO}(\text{C}_6\text{H}_4)\text{O}^-$ .

$m$ -fluorophenol and  $m$ -aminophenol) have been spatially separated, because of their different dipole moments, and have been exploited for a variety of conformer-specific experiments.<sup>9,10,20,21</sup>

Our experiment was carried out using a high-resolution PE imaging apparatus<sup>22</sup> equipped with an ESI source,<sup>23</sup> a temperature-controlled cryogenic ion trap,<sup>24</sup> and a time-of-flight mass spectrometer. The  $m\text{-HO}(\text{C}_6\text{H}_4)\text{O}^-$  anions were produced by ESI of a 1 mM solution of  $m\text{-HO}(\text{C}_6\text{H}_4)\text{OH}$  dissolved in a mixed water/methanol (1:9 ratio) solution at pH  $\sim 8$ . Anions from the ESI source were transferred by two sets of quadrupole ion guide and one octupole ion guide to a cryogenically cooled Paul trap,<sup>24</sup> where they were accumulated and cooled for 0.1 s before being ejected into the extraction zone of a time-of-flight mass spectrometer. The desirable  $m\text{-HO}(\text{C}_6\text{H}_4)\text{O}^-$  anions were mass-selected and focused into a colinear velocity-map imaging lens system,<sup>22</sup> where they were intercepted by a linearly polarized laser beam from a dye laser. Photoelectrons were projected onto a position-sensitive detector consisting of a pair of 75 mm diameter microchannel plates coupled to a phosphor screen and captured by a charge-coupled-device camera. The recorded PE images were inverse-Abel transformed to obtain three-dimensional photoelectron distributions using pBASEX.<sup>25</sup> The imaging system was calibrated using the known spectrum of  $\text{Au}^-$ . All the experiments were performed by operating the ion trap at 4.4 K to completely eliminate vibrational hot bands and minimize rotational broadening.<sup>15–19</sup> The PE spectral resolution achieved was  $3.8\text{ cm}^{-1}$  at  $55\text{ cm}^{-1}$  KE electrons and about 1.5% ( $\Delta\text{KE}/\text{KE}$ ) for KE above 1 eV.

Figure 2 shows the PE image and spectrum of  $m\text{-HO}(\text{C}_6\text{H}_4)\text{O}^-$  at 519.80 nm, which reveals three vibrational peaks labeled as  $^S0_0^0$ ,  $^A0_0^0$  and  $^S23_0^1$ . Their binding energies are given in Supporting Information Table S1. The spacing between peaks  $^S0_0^0$  and  $^A0_0^0$  is  $67\text{ cm}^{-1}$ , which is much smaller than the lowest calculated vibrational frequency for both radical

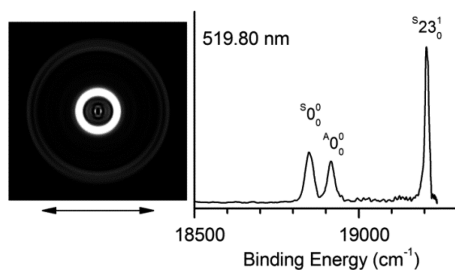


**Figure 2.** Photoelectron image and spectrum of  $m\text{-HO}(\text{C}_6\text{H}_4)\text{O}^-$  taken at 519.80 nm. The double arrow below the image indicates the laser polarization. The superscripts S and A in the labels refer to the *syn* and *anti* conformers, respectively.

conformers, i.e.,  $183\text{ cm}^{-1}$  (Table S2). Clearly, these two peaks represent the origin detachment transitions for the two conformers of  $m\text{-HO}(\text{C}_6\text{H}_4)\text{O}^-$ . A previous theoretical calculation suggested that the electron affinity (EA) of *syn*  $m\text{-HO}(\text{C}_6\text{H}_4)\text{O}\bullet$  is  $120\text{ cm}^{-1}$  lower than that of *anti*  $m\text{-HO}(\text{C}_6\text{H}_4)\text{O}\bullet$ .<sup>26</sup> Thus, we assign the lowest binding energy peak at  $18850\text{ cm}^{-1}$  to the *syn* conformer ( $^S0_0^0$ ) and the peak at  $18917\text{ cm}^{-1}$  to the *anti* conformer ( $^A0_0^0$ ). These values represent the EAs of the two conformers of the  $m\text{-HO}(\text{C}_6\text{H}_4)\text{O}\bullet$  radical, compared with a previous value of 2.330 eV ( $18800\text{ cm}^{-1}$ ) using low-resolution PES, in which conformers were not resolved.<sup>26</sup> The strong peak observed at  $19207\text{ cm}^{-1}$ , which is separated from the  $^S0_0^0$  peak by  $357\text{ cm}^{-1}$  and from the  $^A0_0^0$  peak by  $290\text{ cm}^{-1}$ , should correspond to a vibrational peak of one of the conformers. Since the anion and radical conformers are all planar, this should correspond to an in-plane mode ( $a'$  symmetry). Based on the calculated vibrational frequencies given in Table S2, this peak is readily assigned to the  $\nu_{23}(a')$  mode of *syn*  $m\text{-HO}(\text{C}_6\text{H}_4)\text{O}\bullet$  with a calculated frequency of  $346\text{ cm}^{-1}$  and hence labeled as  $^S23_0^1$ . It should be pointed out that the relative intensity of the  $^S23_0^1$  peak has a significant threshold enhancement and does not reflect the Franck–Condon distribution, as shown in our recent studies.<sup>15–19</sup> Much higher photon energies are needed to obtain PE spectra that reflect the normal Franck–Condon profiles, as shown in the previous lower resolution PE spectra.<sup>26</sup>

To search for excited DBSs of  $m\text{-HO}(\text{C}_6\text{H}_4)\text{O}^-$ , we scanned the dye laser near the detachment thresholds by monitoring the total electron yield, as shown in Figure 3. The  $^S\text{EA}$  and  $^A\text{EA}$

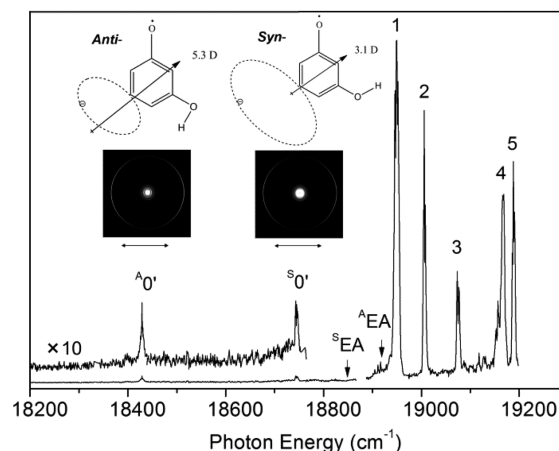


**Figure 3.** Photodetachment spectrum of  $m\text{-HO}(\text{C}_6\text{H}_4)\text{O}^-$  by monitoring the total electron yield as a function of photon energy near the detachment threshold.  $^S\text{EA}$  and  $^A\text{EA}$  indicate the electron affinities of the *syn* and *anti* conformers of  $m\text{-HO}(\text{C}_6\text{H}_4)\text{O}\bullet$ , respectively. The resonant two-photon photoelectron images and the schematic structures of the dipole-bound ground states of the two conformers are shown above the  $^A0'$  and  $^S0'$  peaks.

indicate the EAs of the *syn* and *anti* conformers of  $m\text{-HO}(\text{C}_6\text{H}_4)\text{O}\bullet$ . The continuous signals forming the overall baseline above the thresholds represent direct photodetachment from the ground vibrational states of both anion conformers to their respective neutral ground states. Five intense peaks (labeled as 1–5) are observed, providing evidence of the existence of DBSs as reported recently.<sup>16–19</sup> As shown in the inset of Figure 3, both conformers of  $m\text{-HO}(\text{C}_6\text{H}_4)\text{O}\bullet$  have large enough dipole moments to support

DBSs.<sup>11</sup> Therefore, peaks 1–5 are due to autodetachment from excited vibrational levels of the DBSs of the *m*-HO(C<sub>6</sub>H<sub>4</sub>)O<sup>-</sup> conformers.

To search for the ground vibrational levels of the DBSs, we scanned the dye laser below the detachment thresholds to look for resonant two-photon detachment. Indeed, two very weak peaks labeled as <sup>A</sup>0' and <sup>S</sup>0' at 18 427 cm<sup>-1</sup> and 18 746 cm<sup>-1</sup> are observed below the detachment thresholds. The separation of the two peak (319 cm<sup>-1</sup>) does not correspond to any vibrational frequencies calculated for the two conformers (Table S2), suggesting that they each represent the DBS ground states of the two conformers of *m*-HO(C<sub>6</sub>H<sub>4</sub>)O<sup>-</sup>. Because the dipole moment of the *anti* conformer of *m*-HO(C<sub>6</sub>H<sub>4</sub>)O• (5.3 D) is larger than that of the *syn* conformer (3.1 D), we assign the peak at 18 427 cm<sup>-1</sup> to the DBS origin of the *anti* conformer (<sup>A</sup>0'), giving rise to a DBS binding energy of 490 cm<sup>-1</sup> relative to the detachment threshold of the *anti* conformer (18 917 cm<sup>-1</sup>), as shown in Figure 4. The peak at

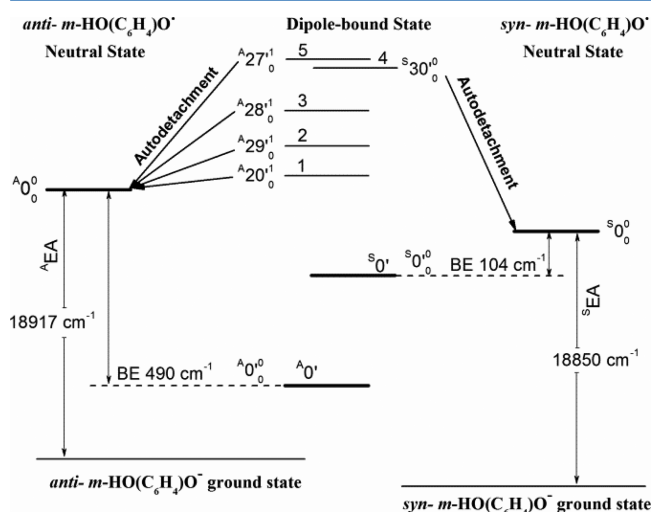


**Figure 4.** Schematic energy level diagram for direct detachment from the ground states of the *anti* and *syn* conformers of *m*-HO(C<sub>6</sub>H<sub>4</sub>)O<sup>-</sup> to those of the corresponding neutral radicals and the autodetachment (represented by the arrows) from the five dipole-bound vibrational states observed in Figure 3. The binding energy (BE) of the dipole-bound state of each conformer is indicated.

18 746 cm<sup>-1</sup> is assigned to the DBS origin of the *syn* conformer (<sup>S</sup>0'), yielding a DBS binding energy of 104 cm<sup>-1</sup> relative to the detachment threshold of the *syn* conformer (18 850 cm<sup>-1</sup>). We measured the PE images corresponding to these two weak peaks, as shown in the inset of Figure 3. The outer ring in each PE image corresponds to single color two-photon detachment. The *p*-wave angular distribution in each case is consistent with the fact that the DBS is analogous to an *s*-type orbital.<sup>16–19</sup> The resonant photon energies for all the vibrational peaks observed in the photodetachment spectrum in Figure 3 are given in Table 1, along with their assignments. As we showed previously,<sup>15–19</sup> the vibrational frequencies of the DBSs of the anions are the same as the corresponding neutral radicals because the electron in the DBS has very little effect on the neutral core. The assignments for peaks 1–5 are all based on and supported by resonant PE spectra to be presented next in Figure 5, in addition to the comparison with the calculated frequencies for both radical conformers in Table S2.

**Table 1.** Observed Photon Energy ( $h\nu$ ), Shifts from the 0' Peaks, and Assignments of the Vibrational Autodetachment Resonances in Figure 3<sup>a</sup>

peak	$h\nu$ (cm <sup>-1</sup> ) <sup>b</sup>	shift (cm <sup>-1</sup> )	assignment
<sup>A</sup> 0'	18 427(5)	<sup>A</sup> 0	<sup>A</sup> 0' <sub>0</sub> <sup>0</sup>
<sup>S</sup> 0'	18 746(5)	<sup>S</sup> 0	<sup>S</sup> 0' <sub>0</sub> <sup>0</sup>
1	18 949(5)	<sup>A</sup> 522	<sup>A</sup> 20' <sub>0</sub> <sup>1</sup>
2	19 006(5)	<sup>A</sup> 579	<sup>A</sup> 29' <sub>0</sub> <sup>1</sup>
3	19 073(5)	<sup>A</sup> 646	<sup>A</sup> 28' <sub>0</sub> <sup>1</sup>
4	19 168(5)	<sup>S</sup> 422	<sup>S</sup> 30' <sub>0</sub> <sup>1</sup>
5	19 188(5)	<sup>A</sup> 761	<sup>A</sup> 27' <sub>0</sub> <sup>1</sup>

<sup>a</sup>Note that the superscripts S and A refer to the *syn* and *anti* conformers, respectively. <sup>b</sup>The number in the parentheses indicates the experimental uncertainty in the last digit.

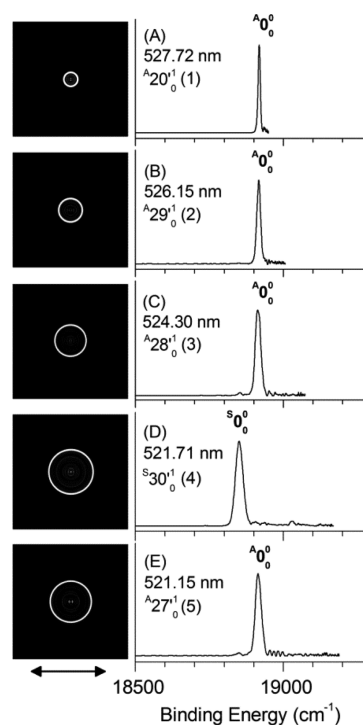


**Figure 5.** Resonant photoelectron images and spectra of *m*-HO(C<sub>6</sub>H<sub>4</sub>)O<sup>-</sup> at five different detachment wavelengths. The numbers in the parentheses correspond to the resonant peaks in Figure 3 and the corresponding vibrational levels of the DBSs are given in each spectrum. The superscripts S and A in the labels refer to the *syn* and *anti* conformers, respectively.

It is interesting that four of the five vibrational resonances observed in Figure 3 belong to the *anti* isomer, whereas only one is from the *syn* conformer. This is due to the very different binding energies of the DBS of the two conformers, which led to very different accessible vibrational levels at the same excitation photon energy. This can be easily understood using the energy level diagram shown in Figure 4. The *anti* conformer has a much larger binding energy, and its DBS vibrational ground state is measured at 18 427 cm<sup>-1</sup> (Figure 3 and Table 1). Since the highest excitation photon energy we used was 19 200 cm<sup>-1</sup> (Figure 3), the accessible vibrational excitation for the DBS of the *anti* conformer was 773 cm<sup>-1</sup> (19 200 cm<sup>-1</sup> – 18 427 cm<sup>-1</sup>). However, the vibrational ground state of the DBS of the *syn* conformer is at 18 746 cm<sup>-1</sup>, which gives rise to a much lower accessible vibrational excitation of 454 cm<sup>-1</sup> at

the highest excitation photon energy of  $19\,200\text{ cm}^{-1}$  ( $19\,200\text{ cm}^{-1} - 18\,746\text{ cm}^{-1}$ ). Thus, many more vibrational levels of the *anti* conformer were expected to be observed, as born out experimentally.

When tuning the detachment laser to the above-threshold peaks (1–5) observed in Figure 3, we obtained resonantly enhanced PE spectra due to autodetachment from a single conformer of  $m\text{-HO}(\text{C}_6\text{H}_4)\text{O}^-$ , as shown in Figure 5. Each PE spectrum contains contribution from both the conventional nonresonant photodetachment (negligible) and resonantly enhanced vibrational autodetachment via the DBS, leading to totally different vibrational patterns from Figure 2. Specifically, Figure 5a–c,e shows that peak  $A^0_0$  is dramatically enhanced, and the  $S^0_0$  peak is negligible. The spectrum in Figure 5a gives the most accurate measurement for the EA of the *anti* conformer, as given in Table S1. On the other hand, Figure 5d shows that peak  $S^0_0$  is dominantly enhanced, and the  $A^0_0$  peak is negligible.

Vibrational autodetachment from DBSs obeys the  $\Delta v = -1$  propensity rule,<sup>15,27,28</sup> i.e., the  $n$ th overtone of a given mode ( $\nu^n$ ) of a DBS can only autodetach to the  $(n-1)$ th vibrational level of the same mode ( $\nu^{n-1}$ ) in the neutral final state. Therefore, Figure 5a–c,e implies that the autodetachment is from fundamental excitation ( $\nu^1$ ) of different vibrational modes of the DBS of the *anti* conformer of  $m\text{-HO}(\text{C}_6\text{H}_4)\text{O}^-$ , while Figure 5d corresponds to autodetachment from fundamental excitation of a vibrational mode of the DBS of the *syn* conformer. The assignments of the specific vibrational modes, as given in Figure 5 and Table 1, are made by comparing the experimental frequencies with the calculated frequencies (Table S2).

The autodetachment processes revealed in Figure 5 can be readily understood by the schematic energy level diagram in Figure 4, showing direct detachment from the ground states of both anion conformers to those of the corresponding neutral radicals and the autodetachment from each vibrational level of the DBSs of the two conformers. The EAs of both radical conformers and the binding energies of the DBSs of both anion conformers are also provided. As shown in Figure 4, when a specific DBS vibrational level (middle) of an anion conformer is excited, the final neutral state of the corresponding radical conformer is reached. In this way, *syn* and *anti* conformers of  $m\text{-HO}(\text{C}_6\text{H}_4)\text{O}^-$  can be selected and generate conformation-selective radicals. Because of the dramatic resonant enhancement in the excitation to the DBS vibrational levels and the subsequent fast autodetachment, the direct nonresonant detachment is almost negligible. It would also be possible to produce single conformers of  $m\text{-HO}(\text{C}_6\text{H}_4)\text{O}\bullet$  with well-defined vibrational energies if higher vibrational levels of the DBSs are excited.<sup>15–19</sup> Hence, autodetachment via DBSs can be applied to select anions with close conformers and dipolar neutral cores.

## ■ ASSOCIATED CONTENT

### Supporting Information

Measured binding energies from the photoelectron spectra of  $m\text{-HO}(\text{C}_6\text{H}_4)\text{O}^-$  and the calculated vibrational frequencies of the *syn* and *anti* conformers of the  $m\text{-HO}(\text{C}_6\text{H}_4)\text{O}\bullet$  radical. The Supporting Information is available free of charge on the ACS Publications website at DOI: 10.1021/acs.jpcllett.5b00963.

## ■ AUTHOR INFORMATION

### Corresponding Author

\*E-mail: Lai-Sheng\_Wang@brown.edu.

### Notes

The authors declare no competing financial interests.

## ■ ACKNOWLEDGMENTS

This work was supported by the National Science Foundation (CHE-1263745 to L.S.W.). C.G.N would like to acknowledge support of NSFC (91336104) and MOST (2013CB922004).

## ■ REFERENCES

- (1) Simons, J. P.; Jockusch, R. A.; Carcabal, P.; Hung, I.; Kroemer, R. T.; Macleod, N. A.; Snoek, L. C. Sugars in the Gas Phase. Spectroscopy, Conformation, Hydration, Co-operativity and Selectivity. *Int. Rev. Phys. Chem.* **2005**, *24*, 489–531.
- (2) de Vries, M. S.; Hobza, P. Gas-Phase Spectroscopy of Biomolecular Building Blocks. *Annu. Rev. Phys. Chem.* **2007**, *58*, 585–612.
- (3) Park, S. T.; Kim, S. K.; Kim, M. S. Observation of Conformation-Specific Pathways in the Photodissociation of 1-Iodopropane Ions. *Nature* **2002**, *415*, 306–308.
- (4) Kim, M. H.; Shen, L.; Tao, H. L.; Martinez, T. J.; Suits, A. G. Conformationally Controlled Chemistry: Excited-State Dynamics Dictate Ground-State Reaction. *Science* **2007**, *315*, 1561–1565.
- (5) Dian, B. C.; Clarkson, J. R.; Zwier, T. S. Direct Measurement of Energy Thresholds to Conformational Isomerization in Tryptamine. *Science* **2004**, *303*, 1169–1173.
- (6) Dian, B. C.; Brown, G. G.; Douglass, K. O.; Pate, B. H. Measuring Picosecond Isomerization Kinetics via Broadband Microwave Spectroscopy. *Science* **2008**, *320*, 924–928.
- (7) Gerlich, D. Inhomogeneous RF-Fields - A Versatile Tool for the Study of Processes with Slow Ions. *Adv. Chem. Phys.* **1992**, *82*, 1–176.
- (8) Rizzo, T. R.; Stearns, J. A.; Boyarkin, O. V. Spectroscopic Studies of Cold, Gas-Phase Biomolecular Ions. *Int. Rev. Phys. Chem.* **2009**, *28*, 481–515.
- (9) Filsinger, F.; Erlekam, U.; von Helden, G.; Kupper, J.; Meijer, G. Selector for Structural Isomers of Neutral Molecules. *Phys. Rev. Lett.* **2008**, *100*, 133003.
- (10) Chang, Y. P.; Dlugolecki, K.; Kupper, J.; Rosch, D.; Wild, D.; Willitsch, S. Specific Chemical Reactivities of Spatially Separated 3-Aminophenol Conformers with Cold  $\text{Ca}^+$  Ions. *Science* **2013**, *342*, 98–101.
- (11) Garrett, W. R. Critical Binding of an Electron to a Rotationally Excited Dipolar System. *Phys. Rev. A* **1971**, *3*, 961–972.
- (12) Desfrancois, C.; Baillon, B.; Schermann, J. P.; Arnold, S. T.; Hendricks, J. H.; Bowen, K. H. Prediction and Observation of a New, Ground-State, Dipole-Bound Dimer Anion - The Mixed Water Ammonia System. *Phys. Rev. Lett.* **1994**, *72*, 48–51.
- (13) Zimmerman, A. H.; Brauman, J. I. Resonances in Electron Photodetachment Cross-Sections. *J. Chem. Phys.* **1977**, *66*, 5823–5825.
- (14) Lykke, K. R.; Mead, R. D.; Lineberger, W. C. Observation of Dipole-Bound States of Negative-Ions. *Phys. Rev. Lett.* **1984**, *52*, 2221–2224.
- (15) Liu, H. T.; Ning, C. G.; Huang, D. L.; Dau, P. D.; Wang, L. S. Observation of Mode-Specific Vibrational Autodetachment from Dipole-Bound States of Cold Anions. *Angew. Chem., Int. Ed.* **2013**, *52*, 8976–8979.
- (16) Liu, H. T.; Ning, C. G.; Huang, D. L.; Wang, L. S. Vibrational Spectroscopy of the Dehydrogenated Uracil Radical by Autodetachment of Dipole-Bound Excited States of Cold Anions. *Angew. Chem., Int. Ed.* **2014**, *53*, 2464–2468.
- (17) Huang, D. L.; Zhu, G. Z.; Wang, L. S. Observation of Dipole-Bound State and High-Resolution Photoelectron Imaging of Cold Acetate Anions. *J. Chem. Phys.* **2015**, *142*, 091103.

(18) Huang, D. L.; Liu, H. T.; Ning, C. G.; Wang, L. S. Vibrational State-Selective Autodetachment Photoelectron Spectroscopy from Dipole-Bound States of Cold 2-Hydroxyphenoxide:  $o\text{-HO}(\text{C}_6\text{H}_4)\text{O}^-$ . *J. Chem. Phys.* **2015**, *142*, 124309.

(19) Huang, D. L.; Liu, H. T.; Ning, C. G.; Zhu, G. Z.; Wang, L. S. Probing the Vibrational Spectroscopy of the Deprotonated Thymine Radical by Photodetachment and State-Selective Autodetachment Photoelectron Spectroscopy via Dipole-Bound States. *Chem. Sci.* **2015**, *6*, 3129–3138.

(20) Filsinger, F.; Meijer, G.; Stapelfeldt, H.; Chapman, H. N.; Kupper, J. State- and Conformer-Selected Beams of Aligned and Oriented Molecules for Ultrafast Diffraction Studies. *Phys. Chem. Chem. Phys.* **2011**, *13*, 2076–2087.

(21) Rosch, D.; Willitsch, S.; Chang, Y. P.; Kupper, J. Chemical Reactions of Conformationally Selected 3-Aminophenol Molecules in a Beam with Coulomb-Crystallized  $\text{Ca}^+$  Ions. *J. Chem. Phys.* **2014**, *140*, 124202.

(22) Leon, I.; Yang, Z.; Liu, H. T.; Wang, L. S. The design and Construction of a High-Resolution Velocity-Map Imaging Apparatus for Photoelectron Spectroscopy Studies of Size-Selected Clusters. *Rev. Sci. Instrum.* **2014**, *85*, 083106.

(23) Wang, L. S.; Ding, C. F.; Wang, X. B.; Barlow, S. E. Photodetachment Photoelectron Spectroscopy of Multiply Charged Anions Using Electrospray Ionization. *Rev. Sci. Instrum.* **1999**, *70*, 1957–1966.

(24) Wang, X. B.; Wang, L. S. Development of a Low-Temperature Photoelectron Spectroscopy Instrument Using an Electrospray Ion Source and a Cryogenically Controlled Ion Trap. *Rev. Sci. Instrum.* **2008**, *79*, 073108.

(25) Garcia, G. A.; Nahon, L.; Powis, I. Two-Dimensional Charged Particle Image Inversion Using a Polar Basis Function Expansion. *Rev. Sci. Instrum.* **2004**, *75*, 4989–4996.

(26) Wang, X. B.; Fu, Q.; Yang, J. Electron Affinities and Electronic Structures of *o*-, *m*-, and *p*-Hydroxyphenoxy Radicals: A Combined Low-Temperature Photoelectron Spectroscopic and Ab Initio Calculation Study. *J. Phys. Chem. A* **2010**, *114*, 9083–9089.

(27) Berry, R. S. Ionization of Molecules at Low Energies. *J. Chem. Phys.* **1966**, *45*, 1228–1245.

(28) Simons, J. Propensity Rules for Vibration-Induced Electron Detachment of Anions. *J. Am. Chem. Soc.* **1981**, *103*, 3971–3976.